

Probing the $W'_L WH$ and $W'_R WH$ interactions at LHCShou-Shan Bao,^{1,*} Hong-Lei Li,^{1,†} Zong-Guo Si,^{1,2,‡} and Yu-Feng Zhou^{3,§}¹*School of Physics, Shandong University, Jinan Shandong 250100, People's Republic of China*²*Center for High-Energy Physics, Peking University, Beijing 100871, People's Republic of China*³*Kavli Institute for Theoretical Physics China (KITPC), Key Laboratory of Frontiers in Theoretical Physics, Institute of Theoretical Physics, Chinese Academy of Science, Beijing, 100190, People's Republic of China*

(Received 9 March 2011; revised manuscript received 29 April 2011; published 1 June 2011)

Many new physics models predict the existence of TeV-scale charged gauge boson W' together with Higgs-boson(s). We study the $W'WH$ interaction and explore the angular distribution of charged leptons to distinguish $W'_R WH$ from $W'_L WH$ in the $pp \rightarrow HW \rightarrow b\bar{b}l\nu$ process at the LHC. It is found that a new type forward-backward asymmetry (A_{FB}) relating to the angle between the direction of the charged lepton in the W rest frame and that of the reconstructed W' in the laboratory frame is useful to investigate the properties of $W'WH$ interaction. We analyze the standard model backgrounds and develop a set of cuts to highlight the signal and suppress the backgrounds at LHC. We find that A_{FB} can reach 0.03(−0.07) for $W'_R(W'_L)$ production at $\sqrt{S} = 14$ TeV.

DOI: 10.1103/PhysRevD.83.115001

PACS numbers: 12.60.Cn, 11.80.Cr, 14.70.Fm, 14.70.Pw

I. INTRODUCTION

Although the standard model (SM) of particles is extremely successful in phenomenology, there are remaining problems not well understood, such as the gauge hierarchy problem, the origins of fermion masses, mixing and P/CP violation etc. The SM fails to explain the baryon-antibaryon asymmetry in the universe and cannot provide a viable dark matter candidate. It is commonly believed that the SM can only be a low energy effective theory of a more fundamental theory. There already exists various well-motivated new physics models beyond the SM, such as the supersymmetric models [1–3], models with extra dimensions [4–7], the little Higgs models [8–11] and the left-right symmetric models (LRSMs) [12–16], etc. Most new physics models introduce new heavy particles, such as the new neutral (Z') and charged (W') gauge bosons, etc. The signals of these new gauge bosons at the LHC have been extensively studied [17–24]. If the new particles beyond SM are discovered, one needs to go a step further to know their properties such as masses and couplings to the SM particles. In a recent analysis [25], it has been shown that the chirality of the charged gauge boson to the SM fermions can be determined by an angular distribution asymmetry of the final state leptons in the process $pp \rightarrow W'_{L,R} \rightarrow t\bar{b}$ followed by $t \rightarrow bl\nu$, which is useful in distinguishing different new physics models.

Of course, one of the primary goals of the LHC is to discover the light Higgs boson which is essential for testing the electroweak symmetry breaking in the SM. In proton-proton collision, the gluon fusion, $gg \rightarrow H$, is the

dominant channel for Higgs-boson production throughout the Higgs mass range in the SM. Current electroweak fits, together with the LEP exclusion limit, favor a light Higgs around 120 GeV [26], where $H \rightarrow b\bar{b}$ decay mode is dominated. However $gg \rightarrow H \rightarrow b\bar{b}$ is overwhelmed by the large QCD backgrounds. Thus the rare channel $gg \rightarrow H \rightarrow \gamma\gamma$ is explored to be a golden channel for light Higgs searching at LHC due to the clean background. There are also other important Higgs-boson production processes, such as vector boson fusion and the associated production with $t\bar{t}$, W^\pm and Z , etc. A detailed review can be found in [27]. Once a light Higgs boson is found, one still needs to know if it belongs to the SM or some other new physics models, as many new physics models contain one or more Higgs bosons which may have different properties such as flavor changing interactions with SM fermions, or coupling to other new particles such as the new gauge bosons W' and Z' .

If both the new gauge bosons and the light Higgs bosons are discovered at the LHC, investigating the possible interaction between them will shed light on the nature of the underlying new physics. A particularly interesting interaction is the coupling of Higgs to the new charged gauge boson W' and the SM charged gauge boson W . In general, this type of coupling appears when the Higgs boson is charged under more than one nonabelian gauge group or there exists mixing between the Higgs bosons of different types. The $W'WH$ coupling appears in various models such as the extra dimension models, the little Higgs models and the left-right symmetry models. But the nature of the W' involved in the interactions may be quite different.

The $W'WH$ coupling is of particular importance in probing the LRSM. Unlike the extra dimension models and the little Higgs models, the W' in the LRSM couples mostly to right-handed SM fermions. The existence of the $W'WH$ interaction arises from the bidoublet nature of the

*ssbao@sdu.edu.cn

†lihl@mail.sdu.edu.cn

‡zgsi@sdu.edu.cn

§yfzhou@itp.ac.cn

Higgs boson which is essential for generating fermion masses in this model.

In this paper we shall focus on searching for the signal of the possible coupling $W'WH$ at the LHC and determining the chirality of W' , which may not only provide complementary information on properties of the W' from other channels such as $W' \rightarrow tb$ but also reveal the nonstandard interactions of the light Higgs boson. We would like to use the following process

$$pp \rightarrow W'(W) \rightarrow HW \rightarrow b\bar{b}l\nu, \quad (1)$$

to explore the $W'WH$ interaction. We show that the chirality of W' coupling to fermions is correlated to the angular distribution of the final charged leptons through the $W'WH$ vertex. A new type of forward-backward asymmetry determined by the angle between the direction of the charged lepton and that of the final particle system indicates the different properties between $W'_R WH$ and $W'_L WH$.

This paper is organized as follows. In Sec. II, we briefly discuss the coupling of $W'WH$ from the LRSM and other models and give the formulas for the differential cross section. The angular correlations of the final states related to the process $q\bar{q}' \rightarrow W'(W) \rightarrow HW \rightarrow b\bar{b}l\nu$ are shown as well. In Sec. III, the numerical results of $pp \rightarrow W(W') \rightarrow HW$ with $H \rightarrow b\bar{b}$, $W \rightarrow l\nu$ are presented. We finally give a short summary in Sec. IV.

II. THEORETICAL FRAMEWORK

A. $W'WH$ vertex in new physic models

The $W'WH$ vertex appears in many new physics models. As an example we first consider the LRSM in which the $W'WH$ coupling strength is large. In the LRSM, the gauge group is expanded to $SU(2)_L \times SU(2)_R \times U(1)_{B-L}$, and the right-handed fermions are doublets under $SU(2)_R$. To obtain the gauge invariant Yukawa interaction, one must introduce at least one Higgs bidoublet

$$\phi = \begin{pmatrix} \phi_1^+ & \phi_1^+ \\ \phi_2^- & \phi_2^0 \end{pmatrix}, \quad (2)$$

which transforms as a doublet under both $SU(2)_L$ and $SU(2)_R$. Therefore, it couples to both the left-handed and right-handed gauge bosons W_L and W_R . In a version of the minimal LRSM [14,28], two higgs triplets $\Delta_{L,R}$ are introduced to break the left-right symmetry and generate the tiny neutrino masses

$$\Delta_L = \begin{pmatrix} \delta_L^+/\sqrt{2} & \delta_L^{++} \\ \delta_L^0 & -\delta_L^+/\sqrt{2} \end{pmatrix}, \quad (3)$$

$$\Delta_R = \begin{pmatrix} \delta_R^+/\sqrt{2} & \delta_R^{++} \\ \delta_R^0 & -\delta_R^+/\sqrt{2} \end{pmatrix}.$$

The vacuum expectation value of the right-handed triplets $\langle \delta_R^0 \rangle = v_R$ breaks the symmetry $SU(2)_L \times SU(2)_R \times U(1)_{B-L}$ to $SU(2)_L \times U(1)_Y$, and the vacuum expectation value of the bidoublet

$$\langle \phi \rangle = \frac{1}{\sqrt{2}} \begin{pmatrix} k_1 & 0 \\ 0 & k_2 \end{pmatrix}, \quad (4)$$

breaks the electroweak gauge symmetry with $k_+ = \sqrt{k_1^2 + k_2^2} \sim 246$ GeV. The minimal LRSM predicts that the masses of charged gauge bosons are

$$M_{1,2}^2 = \frac{g^2}{4} k_+^2 + v_R^2 \mp \sqrt{v_R^4 + 4k_1^2 k_2^2}, \quad (5)$$

with $\tan\beta = k_1/k_2$ and mixing angle $\tan 2\zeta = -2k_1 k_2 / v_R^2$. Barenboim *et al.* obtained an upper bound for the mixing angle $|\zeta| < 0.0333$ from the muon decay [29]. An upper limit of $|\zeta| < 0.005$ on the mixing angle is derived from semileptonic decay data by Wolfenstein [30]. The limit of $\tan\beta$ can be obtained from the following expression

$$\tan 2\zeta = -\frac{2\tan\beta}{1 + \tan^2\beta} \left(\frac{k_+}{v_R}\right)^2 \approx -\frac{2\tan\beta}{1 + \tan^2\beta} \left(\frac{m_W}{m_{W'}}\right)^2. \quad (6)$$

In the case of $m_{W'} = 1$ TeV, the lower limit of $\tan\beta$ is 1.4 for $|\zeta| < 0.003$ [31]. Thus in the LRSM the W' is mostly right-handed, i.e. $W' \approx W'_R$ and $W \approx W_L$.

The couplings of W'_R to the quarks have the following form

$$\mathcal{L} = \frac{g_R}{2\sqrt{2}} V_{ij}^R \bar{q}_i \gamma^\mu (1 + \gamma^5) q_j' W_R'^\mu + \dots + \text{H.c.}, \quad (7)$$

with g_R the coupling constant and V_{ij}^R the right-handed Cabibbo-Kobayashi-Maskawa quark-mixing matrix (CKM) elements. From the Higgs kinetic terms one obtains the $W'WH$ coupling

$$g_{W'_R WH} = g_L g_R k_+ \frac{\tan\beta}{(1 + \tan^2\beta)}. \quad (8)$$

The coupling strength for WWH is $g_{WWH} = g^2 k_+ / 2 \approx g m_W$.

In other models such as extra dimension models and Little Higgs models the extra charged gauge bosons W' couple to left-handed fermions. The coupling strengths are proportional to the left-handed CKM matrix elements.

$$\mathcal{L} = \frac{g_L}{2\sqrt{2}} V_{ij}^L \bar{q}_i \gamma^\mu (1 - \gamma^5) q_j' W_L'^\mu + \dots + \text{H.c.} \quad (9)$$

We parametrized the $W'_L WH$ vertex as

$$W_L'^\pm W^\mp H \rightarrow (-i) R g_{WWH} g^{\mu\nu}, \quad (10)$$

where R is a model-dependent parameter. For simplicity, as an example, we suppose $R = \sin 2\beta$, which provides the identical coupling $g_{W'_R WH} = g_{W'_L WH}$ for $W'_R WH$ and $W'_L WH$ vertexes. We also set $g_L = g_R = g$ and $V_{ij}^L = V_{ij}^R = V_{ij}$.

The W' mass is limited by both the experimental results and theoretical analysis [32]. A W' boson with mass less than 788 GeV and 800 GeV is excluded by CDF through the decays $W' \rightarrow l\nu$ [33] and $W' \rightarrow t\bar{b}$ [34]. The D0 collaboration obtains a lower bound at 1 TeV for a SM-like W' [35]. A global fit result [36], considering the Fermi constant, Z -mass, etc., shows the lower W' mass bound about 300 GeV. Otherwise, with reasonable fine-tuning restrictions one could obtain $M_{W'} > 300$ GeV [37]. As well as the low energy experiments, i.e., electron-hadron, neutrino-hadron and neutrino-electron processes restrict the mass of W' above 875 GeV [38]. It is pointed out that the neutral current phenomena can provide limits to W' mass [39], and it is summarized in [40] that the W' will be 2–3 TeV. From the $K_L - K_S$ mixing, the W' is limited to above 1.6 TeV [41], and is up to 2.45 TeV including CP -violation restrictions [42,43]. The constraint from neutral K meson mass difference Δm_K demonstrates that the W' mass well below 1 TeV is allowed due to a cancellation caused by a light charged Higgs boson [44], while it is improved to 2.5 TeV and 4 TeV from Δm_B and neutron electric dipole moment constraints [45–47].

B. HW production via $q\bar{q}'$ annihilation

The search for Higgs particles is one of the most important endeavors at LHC. Various channels can be exploited at hadron colliders to search for a Higgs boson.

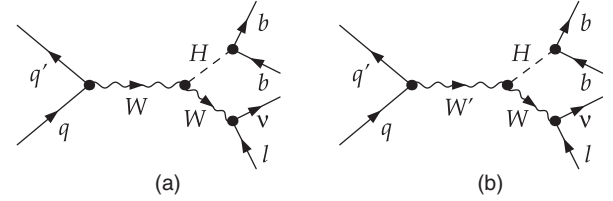


FIG. 1. Lowest-order Feynman diagram at the tree level for process (12) and (13).

In addition to $gg \rightarrow H \rightarrow \gamma\gamma$, Higgs-boson production in association with W or Z bosons through $q\bar{q}'$ annihilation,

$$pp \rightarrow HV + X(H \rightarrow b\bar{b}, V = W \text{ or } Z), \quad (11)$$

is another promising discovery channel for a SM Higgs particle with mass below about 135 GeV [32,48–52]. If a W' boson exits, it will enhance the cross-section around W' mass. In this paper we study the properties of $W'WH$ interaction via the following processes (Fig. 1),

$$q(p_q)\bar{q}'(p_{\bar{q}}) \rightarrow W^+ \rightarrow HW^+ \rightarrow b(p_b)\bar{b}(p_{\bar{b}})l^+(p_l)\nu(p_\nu), \quad (12)$$

$$q(p_q)\bar{q}'(p_{\bar{q}}) \rightarrow W'^+ \rightarrow HW^+ \rightarrow b(p_b)\bar{b}(p_{\bar{b}})l^+(p_l)\nu(p_\nu), \quad (13)$$

where $p_q, p_{\bar{q}}$, etc. respectively denote the 4-momentum of the corresponding particles. H is a SM-like Higgs decaying to $b\bar{b}$ dominantly, thus it can be reconstructed from two b -jets at LHC. The corresponding matrix element square averaged over the spin and color of initial partons is given by

$$|\mathcal{M}|^2 = \frac{2f_{b\bar{b}H}^2 |V_{p\bar{q}'}|^2 (p_b \cdot p_{\bar{b}})}{((s_3 - m_H^2)^2 + \Gamma_H^2 m_H^2)} \left\{ \frac{4g^4 g_{W'WH}^2 (p_q \cdot p_l)(p_{\bar{q}} \cdot p_\nu)}{((s_1 - m_W^2)^2 + \Gamma_W^2 m_W^2)((s_2 - m_W^2)^2 + \Gamma_W^2 m_W^2)} \right. \\ + \frac{g^2 g_{L(R)}^2 g_{W'_{L(R)}WH}^2 [(1+A)^2 (p_q \cdot p_\nu)(p_{\bar{q}} \cdot p_l) + (1-A)^2 (p_q \cdot p_l)(p_{\bar{q}} \cdot p_\nu)]}{((s_1 - m_{W'}^2)^2 + \Gamma_{W'}^2 m_{W'}^2)((s_2 - m_W^2)^2 + \Gamma_W^2 m_W^2)} \\ \left. + \frac{2gg_L g_{W'_L WH} g_{W'WH} (1-A)^2 (p_q \cdot p_l)(p_{\bar{q}} \cdot p_\nu)[(s_1 - m_{W'}^2)(s_1 - m_W^2) + \Gamma_{W'} m_{W'} \Gamma_W m_W]}{((s_1 - m_{W'}^2)^2 + \Gamma_{W'}^2 m_{W'}^2)((s_1 - m_W^2) + \Gamma_W^2 m_W^2)((s_2 - m_W^2) + \Gamma_W^2 m_W^2)} \right\}, \quad (14)$$

where $s_1 = \hat{s} = 2p_q \cdot p_{\bar{q}}$, $s_2 = 2p_l \cdot p_\nu$, $s_3 = 2p_b \cdot p_{\bar{b}}$, $f_{b\bar{b}H}$ is the Yukawa coupling of $b\bar{b}H$ interaction, and $V_{p\bar{q}'}$ is the CKM matrix element. Γ_H, Γ_W and $\Gamma_{W'}$ denote the Higgs, W and W' width, respectively, and the W' width is listed in the Appendix. The first two terms in Eq. (14) stand for the matrix element square for process (12) and (13) respectively, and the third term is their interference term. $A = 1(-1)$ stands for right- (left-) handed W' . Obviously the interference term disappears for the case

of right-handed W' production. The cross section at parton level can be written as

$$\hat{\sigma}(\hat{s}) = \int \frac{|\mathcal{M}|^2}{2\hat{s}} (2\pi)^4 \delta^{(4)}\left(\sum_f p_f - p_q - p_{q'}\right) \prod_f \frac{d^3 p_f}{(2\pi)^3 2E_f}, \quad (15)$$

where $f = b, \bar{b}, l^+, \nu$. From the second term in Eq. (14), one can notice that the angular distribution of the charged

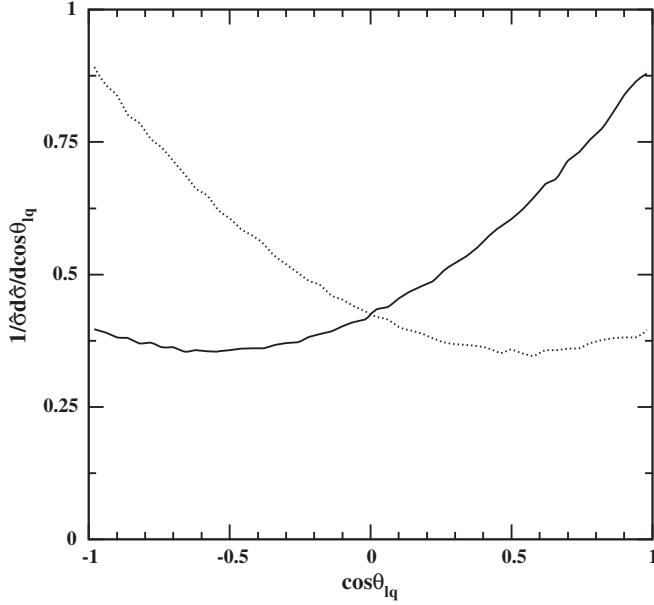
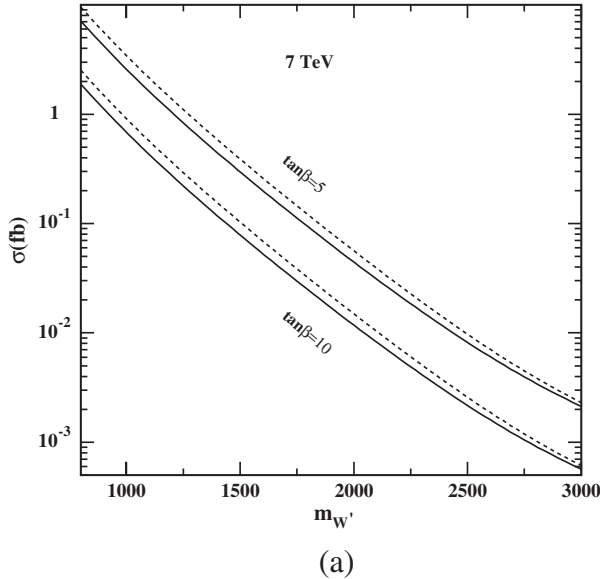


FIG. 2. The angular distribution for the final charged lepton at parton level with $\sqrt{\hat{s}} = 1$ TeV. The solid (dashed) line is the result of the left- (right-) handed W' with $M_{W'} = 1$ TeV.

lepton is different for the left- and right-handed W' bosons. In order to show this point clearly, we define the angle between the 3-momentum \mathbf{p}_l^* of the charged lepton in the W rest frame, and that (\mathbf{p}_q) of the initial quark in the $q\bar{q}'$ center of mass system as

$$\cos\theta_{lq} = \frac{\mathbf{p}_l^* \cdot \mathbf{p}_q}{|\mathbf{p}_l^*| \cdot |\mathbf{p}_q|}. \quad (16)$$



The differential distribution $1/\hat{\sigma} d\hat{\sigma}/d\cos\theta_{lq}$ for the partonic process $q\bar{q}' \rightarrow W' \rightarrow HW \rightarrow b\bar{b}l^+\nu$ at $\sqrt{\hat{s}} = 1$ TeV is displayed in Fig. 2. Obviously, the charged leptons, produced through W'_L (W'_R), tend to move along the direction of the initial antiquark (quark), i.e., the $W'_R WH$ and $W'_L WH$ interaction may be distinguished from this kind of angular distribution.

III. NUMERICAL RESULTS

For the processes

$$pp \rightarrow W'^+(W^+) \rightarrow HW^+ \rightarrow b\bar{b}l^+\nu, \quad (17)$$

the total cross section can be expressed as

$$\sigma = \int dx \int dy q_i(x) \bar{q}_j(y) \hat{\sigma}(\hat{s}), \quad (18)$$

where $q(x)(\bar{q}(y))$ is the parton distribution function of quark (antiquark). CTEQ611 [53] is used in this work. To obtain the numerical results we adopt the parameters limited in the LRSM framework related to the W'_R production. For simplicity we use the same values for W'_L production.

The total cross section for

$$pp \rightarrow W'^+ \rightarrow HW^+ \rightarrow b\bar{b}l^+\nu \quad (19)$$

at LHC versus $m_{W'}$ is shown in Fig. 3. With a luminosity of 100 fb^{-1} at LHC, A W' boson production could be detected with mass up to 2 (3) TeV if $\tan\beta = 10$, and up to 2.5 (4) TeV if $\tan\beta = 5$. The discrepancy between W'_R and W'_L is due to the different total decay widths. The cross section related to $\tan\beta$ for $m_{W'} = 1$ TeV is displayed in Fig. 4. It is found that up to $\tan\beta = 70$, the process (19) might be observed with luminosity of 100 fb^{-1} at LHC.

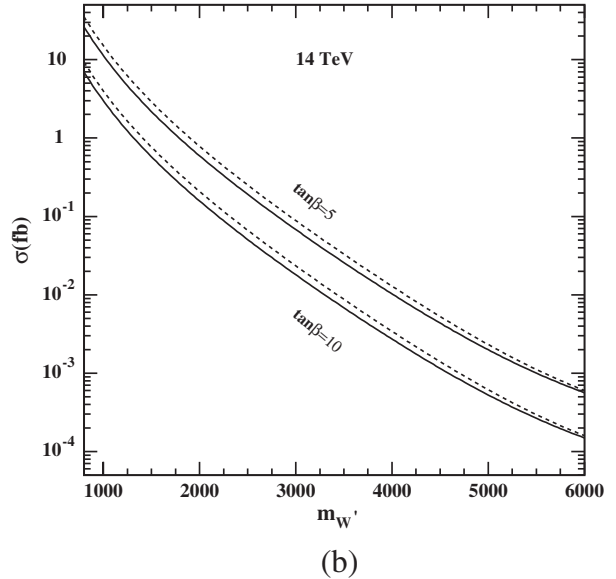


FIG. 3. The total cross section distribution for process $pp \rightarrow W'^+ \rightarrow HW^+ \rightarrow b\bar{b}l^+\nu$ with $m_{W'}$ at LHC for (a) $\sqrt{s} = 7$ TeV and (b) $\sqrt{s} = 14$ TeV. The solid (dashed) lines stand for W'_L (W'_R).

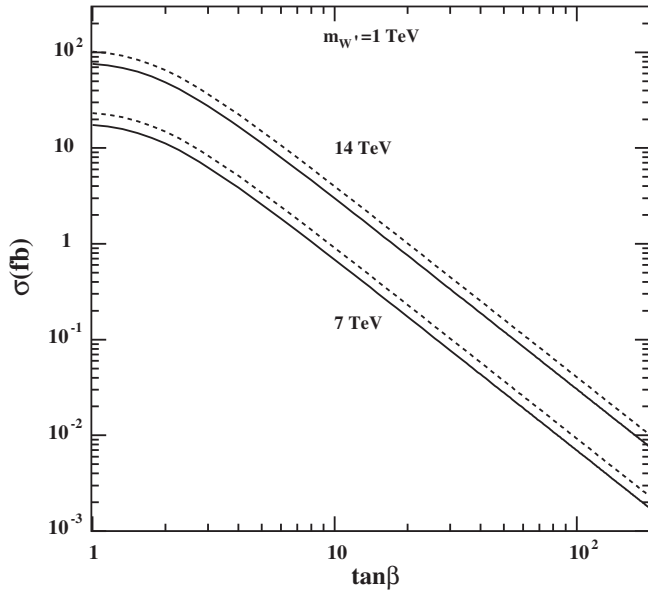


FIG. 4. The total cross section distribution for process $pp \rightarrow W'^+ \rightarrow HW^+ \rightarrow b\bar{b}l^+\nu$ with $\tan\beta$ at LHC. The solid (dashed) lines stand for $W'_L(W'_R)$.

In our following numerical studies, we set $\tan\beta = 5$ and $m_{W'} = 1$ TeV.

Figure 5 shows the differential distribution $d\sigma/dM$ of process (17), where

$$M = \sqrt{(p_b + p_{\bar{b}} + p_{l^+} + p_\nu)^2}. \quad (20)$$

The W' production induces a resonance peak around the W' mass threshold. For the W'_R production, the interference between the W' and W bosons is zero, while for the W'_L the

interference term (Eq. (14)) is negative in the region of $m_W < M < M_{W'}$ which causes a dip in the curve and inversely a positive enhancement to the cross section for the case of $M_R > M_{W'}$. This discrepancy can provide some useful information to distinguish the $W'_L WH$ from $W'_R WH$.

Following the analysis in Sec. II B, we begin to investigate the angular distribution of charged leptons at hadronic level. Since the LHC is a proton-proton collider, the quark can identically come from either proton, and the charged lepton angular distribution will be symmetrized, unless we distinguish the direction of the quark from that of the antiquark. It can be achieved approximately based on the argument that an initial quark takes a larger momentum fraction than an initial antiquark on average, since the former is a valence quark in the proton and the latter a sea quark. Hence the final particle system ($b\bar{b}l^+\nu$) will move along with the initial quark with a large probability. This means one can define the total momentum of final particle system $\mathbf{p} = \mathbf{p}_b + \mathbf{p}_{\bar{b}} + \mathbf{p}_{l^+} + \mathbf{p}_\nu$ instead of the quark's to redefining the charged lepton angular distribution,

$$\cos\theta^* = \frac{\mathbf{p}_l^* \cdot \mathbf{p}}{|\mathbf{p}_l^*| \cdot |\mathbf{p}|}. \quad (21)$$

The differential distribution $1/\sigma d\sigma/d\cos\theta^*$ for the process (19) with $|\mathbf{p}| \neq 0$ is displayed in Fig. 6. It is found that the distributions corresponding to W'_R and W'_L production have different behaviors which may be used to discriminate the $W'_R WH$ and $W'_L WH$ interaction.

To determine the W' chiral coupling from the angular distribution, one must consider the momentum of the final states ($b\bar{b}l^+\nu$). To be as realistic as possible, we simulate the detector performance by smearing the lepton and $b(\bar{b})$

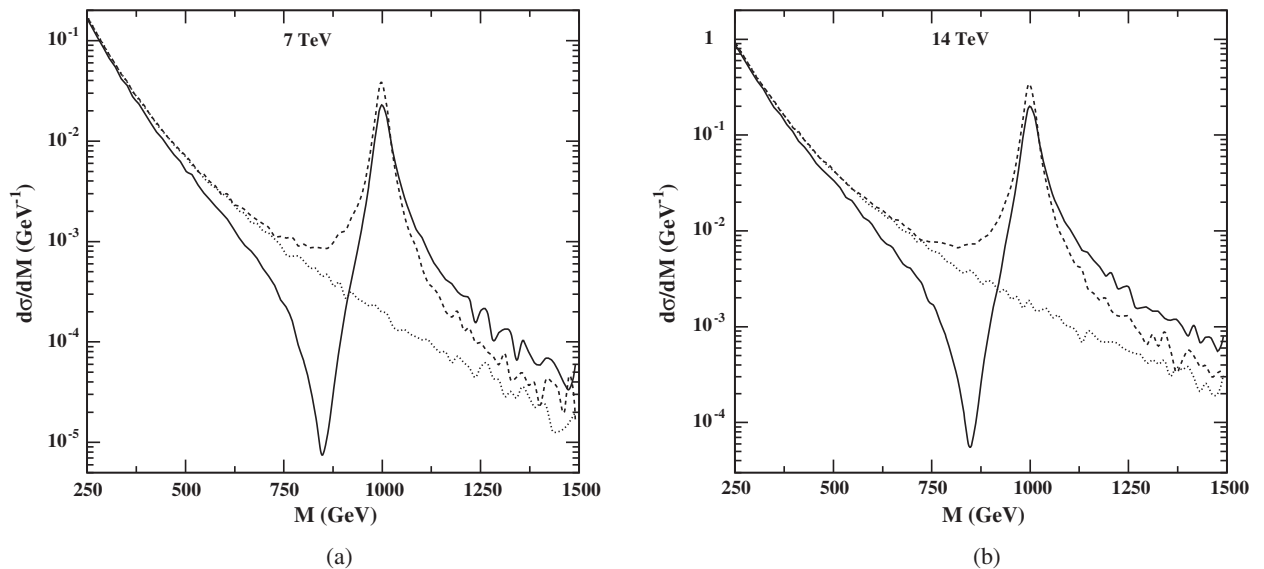


FIG. 5. The differential distribution with M for process $pp \rightarrow HW^+ \rightarrow b\bar{b}l^+\nu$. The solid (dashed) lines are contributed by $W'_L + SM(W'_R + SM)$, and the dotted lines are only the results of SM.

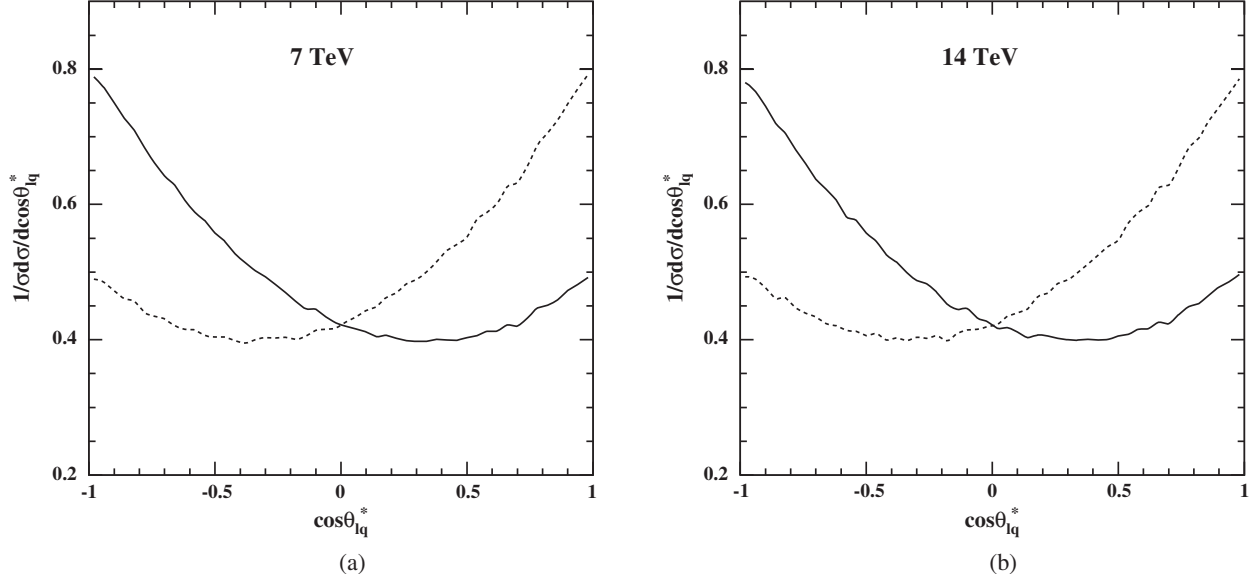


FIG. 6. The angular distribution of the charged lepton for process (19) with $\sqrt{s} = 7$ TeV and 14 TeV. The solid (dashed) lines are the results for W'_L (W'_R).

quark energies according to the assumed Gaussian resolution parametrization

$$\frac{\sigma(E)}{E} = \frac{a}{\sqrt{E}} \oplus b, \quad (22)$$

where $\sigma(E)/E$ is the energy resolution, a is a sampling term, b is a constant term, and \oplus denotes a sum in quadrature. We take $a = 5\%$, $b = 0.55\%$ for leptons and $a = 100\%$, $b = 5\%$ for jets respectively [54]. Since the neutrino is an unobservable particle, one has to utilize kinematical constraints to reconstruct its 4-momentum. Its transverse momentum can be obtained by momentum conservation from the observed particles

$$\mathbf{p}_{\nu T} = -(\mathbf{p}_{lT} + \mathbf{p}_{bT} + \mathbf{p}_{\bar{b}T}), \quad (23)$$

but the longitudinal momentum can not be determined in this way due to the unknown boost of the partonic c.m. system. Alternatively, it can be solved with twofold ambiguity through the on shell condition for the W -boson

$$m_W^2 = (p_\nu + p_l)^2. \quad (24)$$

Furthermore one can impose the on shell condition for the W' -boson to remove the ambiguity. For each possibility we evaluate the total invariant mass M as defined in Eq. (20) and pick up the solution which is closest to the W' mass. With such a solution, one can reconstruct the 4-momentum of the neutrino.

In our following numerical calculations, we apply the basic acceptance cuts (referred to as cut I)

$$\begin{aligned} p_T(l) &> 50 \text{ GeV}, & |\eta(l)| &< 2.5, \\ p_T(j) &> 50 \text{ GeV}, & |\eta(j)| &< 3.0, \\ E_T &> 50 \text{ GeV}, & |y_c| &> 0.1, \end{aligned} \quad (25)$$

where y_c is the rapidity of the reconstructed W' in the laboratory frame.

To purify the signal, we adopt $|M - M_{W'}| < 100$ GeV and $|M_{b\bar{b}} - M_H| < 10$ GeV as further cuts (referred to as cut II), where $M_{b\bar{b}}$ is the invariant mass of $b\bar{b}$.

In Fig. 7, we display the normalized differential distribution $1/\sigma d\sigma/d\cos\theta^*$ with all above cuts. Though the neutrino reconstruction may reduce the difference of the angular distribution between the W'_L and W'_R production processes, the discrepancy still exists. In order to explore this kind of discrepancy to discriminate the $W'_R WH$ and $W'_L WH$ interaction, we define a forward-backward asymmetry as follows

$$A_{\text{FB}} = \frac{\sigma(\cos\theta^* \geq 0) - \sigma(\cos\theta^* < 0)}{\sigma(\cos\theta^* \geq 0) + \sigma(\cos\theta^* < 0)}. \quad (26)$$

The total cross section together with A_{FB} for process (17) are listed in Table. I at $\sqrt{s} = 7(14)$ TeV. It is found that it is possible to distinguish W'_R from W'_L with cuts. If the luminosity can be accumulated to 300 fb^{-1} at $\sqrt{s} = 14$ TeV, about 1500 events may be found, and A_{FB} can reach $0.03(-0.07)$ for W'_R (W'_L).

Finally, we consider the dominant backgrounds for our signal, i.e., Wbb , WZ and $t\bar{b}$ [55]. The MADGRAPH [56] software package is used in our simulation. The cross sections after each cut are listed in Table. II. Obviously, after all cuts, the total cross section of the dominant backgrounds is much lower than that of the signal.

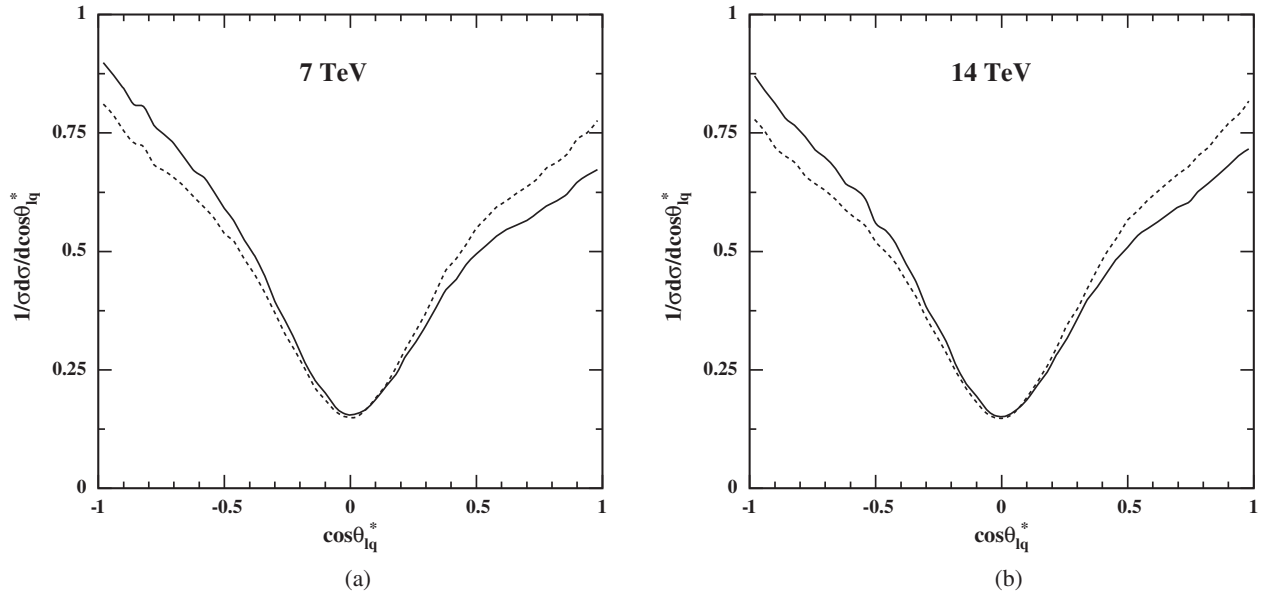


FIG. 7. The angular distribution of charged leptons for process (17) after all cuts with $\sqrt{s} = 7$ TeV and 14 TeV. The solid (dashed) lines are the results for $W'_L(W'_R)$.

IV. SUMMARY

Many theories beyond SM predict the existence of new heavy charged gauge boson W' and searching for Higgs bosons at LHC motivates us to investigate the $W'WH$ interaction. In order to understand its properties, we study the process of $pp \rightarrow W'^+(W^+) \rightarrow HW^+ \rightarrow b\bar{b}l^+\nu$ in this work. Because of the resonance effect of the intermediate W' , there appears a peak in the invariant mass spectrum of the final states, and for the W'_L production, a dip appears in the region of $m_W < M < M'_W$ induced by the interference term. Our numerical results reveal that the angular distribution $d\sigma/d\cos\theta^*$ and the forward-backward

TABLE I. The total cross section and the forward-backward asymmetry before and after cuts with $\sqrt{s} = 7$ TeV and 14 TeV at the LHC.

| | 7 TeV | | | | 14 TeV | | | |
|--------------|--------|--------|------------|--------|--------|--------|------------|--------|
| | no cut | | cut I + II | | no cut | | cut I + II | |
| | W'_L | W'_R | W'_L | W'_R | W'_L | W'_R | W'_L | W'_R |
| $\sigma(fb)$ | 45.9 | 50.3 | 0.97 | 1.38 | 129 | 143 | 4.53 | 6.30 |
| A_{FB} | -0.38 | -0.35 | -0.10 | -0.01 | -0.35 | -0.31 | -0.07 | 0.03 |

TABLE II. The total background cross section after cuts with $\sqrt{s} = 7$ TeV and 14 TeV at the LHC (unit of fb).

| | 7 TeV | | 14 TeV | |
|-------------|-------|------------|--------|------------|
| | cut I | cut I + II | cut I | cut I + II |
| $t\bar{b}$ | 0.61 | 0.005 | 11.2 | 0.01 |
| $Wb\bar{b}$ | 23.9 | 0.04 | 63.8 | 0.08 |
| WZ | 6.69 | 0.01 | 16.6 | 0.02 |

asymmetry A_{FB} can provide helpful information for the $W'WH$ interaction. It is found that for $m_{W'} = 1$ TeV, A_{FB} can reach about 0.03(-0.07) for $W'_R WH(W'_L WH)$ at LHC($\sqrt{s} = 14$ TeV). The backgrounds are estimated and largely suppressed by the kinematical constraints. Once the $W' \rightarrow HW$ process is observed and enough numbers of events are accumulated, our method can be used to study the $W'WH$ interaction and discriminate $W'_R WH$ from $W'_L WH$ so that it is possible to distinguish different new physics models including $W'WH$ interaction.

ACKNOWLEDGMENTS

This work is supported in part by the NSFC and the Natural Science Foundation of Shandong Province (Contract No. JQ200902).

APPENDIX: W' DECAY WIDTH

For estimating the cross section of $q'\bar{q}' \rightarrow W'_{L(R)} \rightarrow HW$, a narrow width approximation is used. The decay width of W' is given in the following parts. In this LRSM we have forbidden W' from decaying into heavy right-handed neutrinos. The width for W' decaying to a pair of quarks is

$$\Gamma(W'_{L(R)} \rightarrow q\bar{q}') = \frac{m_{W'}}{16\pi} |V_{q\bar{q}'}|^2 g^2 g_{L(R)}^2, \quad (A1)$$

$$\begin{aligned} \Gamma(W'_{L(R)} \rightarrow t\bar{b}) &= \frac{m_{W'}}{16\pi} |V_{q\bar{q}'}|^2 g^2 g_{L(R)}^2 \left(1 - \frac{m_t^2}{m_{W'}^2}\right) \\ &\times \left(1 - \frac{m_t^2}{2m_{W'}^2} - \frac{m_t^4}{2m_{W'}^4}\right). \end{aligned} \quad (A2)$$

The width for W' decaying to W -boson and Higgs is

$$\begin{aligned} \Gamma(W'_R \rightarrow HW) \\ = \frac{g_{W'W\phi}^2}{24\pi m_{W'}^2} P_f \left[-6 + \frac{(m_{W'}^2 + m_W^2 - m_\phi^2)^2}{4m_{W'}^2 m_W^2} \right], \end{aligned} \quad (\text{A3})$$

$$\begin{aligned} \Gamma(W'_L \rightarrow HW) \\ = \frac{g_{\text{SM}}^2}{24\pi m_{W'}^2} P_f \left[-6 + \frac{(m_{W'}^2 + m_W^2 - m_\phi^2)^2}{4m_{W'}^2 m_W^2} \right], \end{aligned} \quad (\text{A4})$$

$$P_f = \frac{\sqrt{(m_{W'}^2 - (m_W + m_\phi)^2)(m_{W'}^2 - (m_W - m_\phi)^2)}}{2m_{W'}}, \quad (\text{A5})$$

where the coupling is the same as the SM for W'_L , $g_{\text{SM}} = k_+ g^2/2$. It is left-right symmetry for W'_L and W'_R in the above channel, while this symmetry is violated in the leptonic decay. Because of the heavy mass of the right-handed neutrinos, the W'_R decay to leptons is not allowed. The leptonic decay width is only

$$\Gamma(W'_L \rightarrow l_i \nu_i) = \frac{m_{W'}^2}{48\pi} g^2 g_L^2. \quad (\text{A6})$$

-
- [1] J. Wess and B. Zumino, *Phys. Lett. B* **49**, 52 (1974).
[2] H. E. Haber and G. L. Kane, *Phys. Rep.* **117**, 75 (1985).
[3] S. P. Martin, [arXiv:hep-ph/9709356](https://arxiv.org/abs/hep-ph/9709356).
[4] O. Klein, *Z. Phys.* **37**, 895 (1926); *Surv. High Energy Phys.* **5**, 241 (1986).
[5] N. Arkani-Hamed, S. Dimopoulos, and G. R. Dvali, *Phys. Lett. B* **429**, 263 (1998).
[6] L. Randall and R. Sundrum, *Phys. Rev. Lett.* **83**, 4690 (1999); **83**, 3370 (1999).
[7] N. Arkani-Hamed, A. G. Cohen, and H. Georgi, *Phys. Rev. Lett.* **86**, 4757 (2001).
[8] N. Arkani-Hamed, A. G. Cohen, and H. Georgi, *Phys. Lett. B* **513**, 232 (2001).
[9] N. Arkani-Hamed, A. G. Cohen, E. Katz, A. E. Nelson, T. Gregoire, and J. G. Wacker, *J. High Energy Phys.* **08** (2002) 021.
[10] M. Schmaltz, *Nucl. Phys. B, Proc. Suppl.* **117**, 40 (2003).
[11] T. Han, H. E. Logan, B. McElrath, and L. T. Wang, *Phys. Rev. D* **67**, 095004 (2003).
[12] J. C. Pati and A. Salam, *Phys. Rev. D* **10**, 275 (1974); **11**, 703(E) (1975).
[13] R. N. Mohapatra and J. C. Pati, *Phys. Rev. D* **11**, 566 (1975).
[14] R. N. Mohapatra and J. C. Pati, *Phys. Rev. D* **11**, 2558 (1975).
[15] G. Senjanovic and R. N. Mohapatra, *Phys. Rev. D* **12**, 1502 (1975).
[16] R. N. Mohapatra, F. E. Paige, and D. P. Sidhu, *Phys. Rev. D* **17**, 2462 (1978).
[17] F. I. Olness and M. E. Ebel, *Phys. Rev. D* **30**, 1034 (1984).
[18] D. Feldman, Z. Liu, and P. Nath, *Phys. Rev. Lett.* **97**, 021801 (2006).
[19] K. Agashe *et al.*, *Phys. Rev. D* **76**, 115015 (2007).
[20] K. Agashe, S. Gopalakrishna, T. Han, G. Y. Huang, and A. Soni, *Phys. Rev. D* **80**, 075007 (2009).
[21] J. Galloway, B. McElrath, J. McRaven, and J. Terning, *J. High Energy Phys.* **11** (2009) 031.
[22] K. Agashe, A. Azatov, T. Han, Y. Li, Z. G. Si, and L. Zhu, *Phys. Rev. D* **81**, 096002 (2010).
[23] F. del Aguila, J. de Blas, and M. Perez-Victoria, *J. High Energy Phys.* **09** (2010) 033.
[24] T. J. Gao, T. F. Feng, X. Q. Li, Z. G. Si, and S. M. Zhao, *Sci. China G* **53**, 1988 (2010).
[25] S. Gopalakrishna, T. Han, I. Lewis, Z. G. Si, and Y. F. Zhou, *Phys. Rev. D* **82**, 115020 (2010).
[26] ALEPH Collaboration *et al.* [arXiv:1012.2367](https://arxiv.org/abs/1012.2367).
[27] A. Djouadi, *Phys. Rep.* **457**, 1 (2008).
[28] M. A. B. Beg, R. V. Budny, R. N. Mohapatra, and A. Sirlin, *Phys. Rev. Lett.* **38**, 1252 (1977); **39**, 54(E) (1977).
[29] G. Barenboim, J. Bernabeu, J. Prades, and M. Raidal, *Phys. Rev. D* **55**, 4213 (1997).
[30] L. Wolfenstein, *Phys. Rev. D* **29**, 2130 (1984).
[31] M. Frank, A. Hayreter, and I. Turan, *Phys. Rev. D* **83**, 035001 (2011).
[32] K. Nakamura *et al.* (Particle Data Group), *J. Phys. G* **37**, 075021 (2010).
[33] A. Abulencia *et al.* (CDF Collaboration), *Phys. Rev. D* **75**, 091101 (2007).
[34] T. Aaltonen *et al.* (CDF Collaboration), *Phys. Rev. Lett.* **103**, 041801 (2009).
[35] V. M. Abazov *et al.* (D0 Collaboration), *Phys. Rev. Lett.* **100**, 031804 (2008).
[36] K. Hsieh, K. Schmitz, J. H. Yu, and C. P. Yuan, *Phys. Rev. D* **82**, 035011 (2010).
[37] P. Langacker and S. Uma Sankar, *Phys. Rev. D* **40**, 1569 (1989).
[38] M. Czakon, J. Gluza, and M. Zralek, *Phys. Lett. B* **458**, 355 (1999).
[39] R. N. Mohapatra, G. Senjanovic, and M. D. Tran, *Phys. Rev. D* **28**, 546 (1983).
[40] A. Maiezza, M. Nemevsek, F. Nesti, and G. Senjanovic, *Phys. Rev. D* **82**, 055022 (2010).
[41] G. Beall, M. Bander, and A. Soni, *Phys. Rev. Lett.* **48**, 848 (1982).
[42] G. Ecker and W. Grimus, *Nucl. Phys.* **B258**, 328 (1985).

- [43] Y. Zhang, H. An, X. Ji, and R. N. Mohapatra, *Phys. Rev. D* **76**, 091301 (2007).
- [44] Y.L. Wu and Y.F. Zhou, *Sci. China G* **51**, 1808 (2008).
- [45] Y. Zhang, H. An, X. Ji, and R. N. Mohapatra, *Nucl. Phys.* **B802**, 247 (2008).
- [46] S.Z. Wang, S.Z. Jiang, F.J. Ge, and Q. Wang, *J. High Energy Phys.* **06** (2008) 107.
- [47] S.Z. Wang, F.J. Ge, and Q. Wang, *Phys. Lett. B* **662**, 375 (2008).
- [48] J.M. Butterworth, A.R. Davison, M. Rubin, and G.P. Salam, *Phys. Rev. Lett.* **100**, 242001 (2008).
- [49] A. Del Fabbro and D. Treleani, *Phys. Rev. D* **61**, 077502 (2000).
- [50] A. Stange, W. J. Marciano, and S. Willenbrock, *Phys. Rev. D* **50**, 4491 (1994).
- [51] R. Kleiss, Z. Kunszt, and W. J. Stirling, *Phys. Lett. B* **253**, 269 (1991).
- [52] S.L. Glashow, D.V. Nanopoulos, and A. Yildiz, *Phys. Rev. D* **18**, 1724 (1978).
- [53] J. Pumplin, D.R. Stump, J. Huston, H.L. Lai, P.M. Nadolsky, and W.K. Tung, *J. High Energy Phys.* **07** (2002) 012.
- [54] G. Aad *et al.* (The ATLAS Collaboration), [arXiv:0901.0512](https://arxiv.org/abs/0901.0512).
- [55] Here we do not consider the $pp \rightarrow W'^+ \rightarrow t\bar{b}$ process which is investigated in detail in Ref. [25]. Especially, this process can be largely vetoed by reconstructing the top quark.
- [56] J. Alwall *et al.*, *J. High Energy Phys.* **09** (2007) 028.